Adsorption (2010) 16: 515–523
DOI 10.1007/s10450-010-9264-8

Imaging of transient guest profiles in nanoporous host materials: a new experimental technique to study intra-crystalline diffusion

Christian Chmelik · Jörg Kärger

Published online: 13 August 2010

Abstract The application of interference microscopy (IFM) and infrared microscopy (IRM) to monitoring transient concentration profiles during uptake and release of guest molecules in nanoporous materials has opened a novel technique for diffusion studies with adsorbed molecules. For the first time, the coefficients of transport diffusion and the surface permeabilities have become accessible by direct observation under non-equilibrium conditions. The examples presented in this communication include diffusion and permeation measurements with zeolites of the ferrierite type and with metal-organic frameworks (MOFs) of type ZIF-8

Keywords Diffusion · Zeolites · MOFs · PFG NMR · Interference microscopy · IR microscopy

1 Introduction

Following the example of other fields, our present state of knowledge in adsorption science and technology has been notably formed by the introduction of novel experimental techniques and by the surprises provided by their application to phenomena which, so far, seemed to be well understood. This concerns in particular our understanding of the diffusion of adsorbed molecules. As a first surprise, the introduction of the pulsed field gradient technique of nuclear magnetic resonance (PFG NMR) to zeolitic host-guest systems (Kärger and Caro 1977) showed that, for numerous systems, the intracrystalline diffusivities resulting from this novel type of measurement notably exceeded the values which had hitherto been generally accepted on the basis of macroscopic uptake and release experiments. The progress in our understanding during these days significantly benefitted from the collaboration with Professor Douglas Ruthven. The collaboration resulted in papers on the correlation between "microscopic" and "macroscopic" diffusion measurement (Kärger and Ruthven 1981, 1989) and, eventually, in the "book" on "Diffusion in Zeolites and Other Microporous Solids" (Kärger and Ruthven 1992) which notably influenced the further development in the field .

The novel findings of PFG NMR for molecular self-diffusion (i.e. for the rate of molecular migration under equilibrium conditions) soon found confirmation from quasi-elastic neutron scattering experiments and molecular-dynamic simulations (Jobic and Theodorou 2007). However, irrespective of the novel options of the NMR imaging techniques (Heink et al. 1978; Bär et al. 2000, 2002) for transient sorption experiments with beds of zeolite crystallites, the application of NMR to studying intracrystalline diffusivities was confined to measurements under equilibrium conditions. Eventually, with the introduction of interference microscopy (IFM (Schemmert et al. 1999a, 1999b)) and infra-red microscopy (IRM (Chmelik et al. 2005; Chmelik 2007)), this limitation was overcome and the evolution of concentration profiles within the individual nanoporous crystallites and/or particles has become accessible by direct observation.

In both IFM and IRM, however, sample activation and guest uptake and release have to be performed under the severe spatial confinement brought about by the requirements of optical observation. Thus, the operation and manipulation with a single crystallite in the optical cell turned out to be much more complicated than in corresponding standard experiments with macroscopic samples. In the process of learning all these problems to handle we benefitted a lot

C. Chmelik (✉) · J. Kärger
Faculty of Physics and Geosciences, Leipzig University,
Linnéstr. 5, 04103 Leipzig, Germany
e-mail: chmelik@physik.uni-leipzig.de

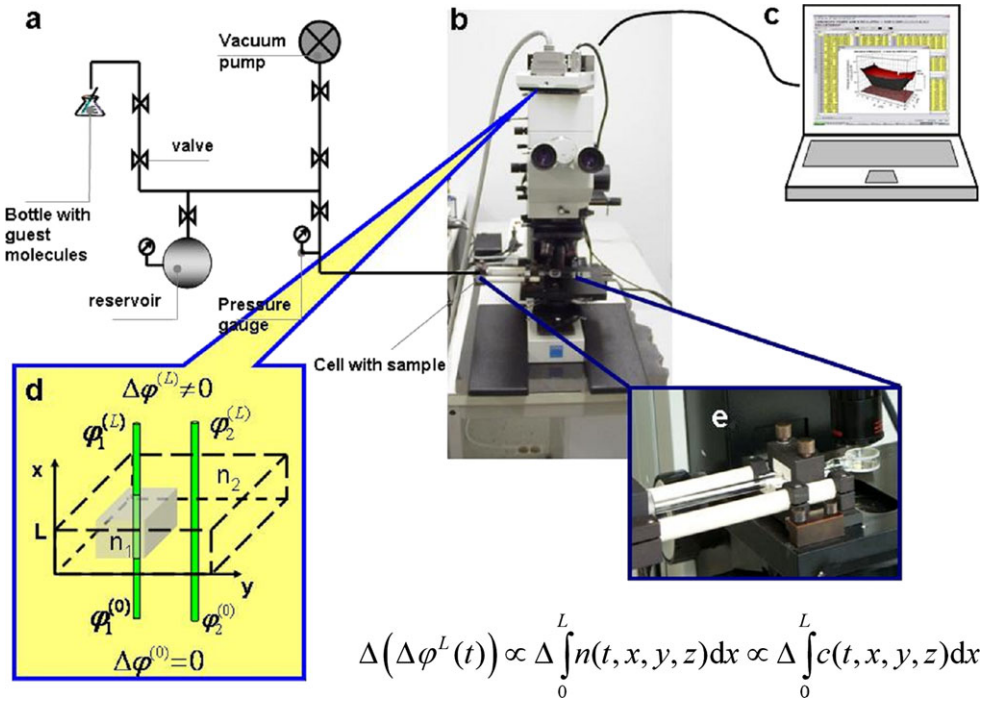

Fig. 1 Experimental set-up and basic principle of the interference microscopy technique for diffusion measurements in nanoporous systems. (**a**) Schematic representation of the vacuum system (static) with optical cell containing the sample. (**b**) Interference microscope with CCD camera on top, directly connected to (**c**) the computer. (**d**) Basic principle: changes in the intracrystalline concentration during diffusion of guest molecules cause changes in the refractive index of the crystal (n_1) and, hence, in the phase difference $\Delta\varphi$ of the two beams. Having measured the difference of the optical path length we can evaluate the difference of the intracrystalline concentration by the given equation. (**e**) Close-up view of the optical cell containing the crystal under study

from Professor Ruthven's presence as a Humboldt Research Awardee in our laboratory in 2003/2004 and from his rich experience in the field. It is, therefore, with great pleasure and gratitude that we dedicated this contribution to Professor Ruthven in deep appreciation of his countless input on our scientific activities.

The paper is organized as follows. After an introduction into the physical foundations of the measuring techniques (Sects. 2.1 and 2.2) and data analysis, the potentials of the novel imaging techniques are highlighted with examples taken from transient sorption studies with zeolite ferrierite (Sect. 3) and with a metal-organic framework (MOF) of type ZIF-8 (Sect. 4).

2 Imaging techniques of transient guest profiles

2.1 Interference microscopy (IFM)

Figure 1 illustrates the way how IFM is applied for the observation of transient concentration profiles in nanoporous materials. The optical cell accommodating the crystal under study (e) is connected with a conventional adsorption/desorption device (a). After activation (by an appropriate programme of temperature increase under permanent evacuation), the sample crystal may thus be subject to any change in the guest pressure in the surrounding atmosphere. This change gives rise to a corresponding change in the guest distribution within the crystal which evolves towards the new equilibrium situation.

A semi-transparent mirror splits the light within the interference microscope (b) into two parallel beams. Figure 1d shows a pair of rays, one (1) passing the crystal under study, the other (2) passing the surrounding atmosphere. In the final image, these two rays are superimposed upon each other. The interference pattern of these two rays is a function of the difference in the optical densities of the crystal and the surrounding atmosphere. By a computer (c), the interference pattern (i.e. the brightness of the given point in the image) may be converted into the corresponding phase differences $\Delta\varphi^L$ between these two rays. The evolution of guest concentration is followed by monitoring the change $\Delta(\Delta\varphi^L)$ in the phase difference $\Delta\varphi^L$. It is indicated by the proportionality relation on the bottom of Fig. 1 that this change is proportional to the change in the integral of the optical density and hence, in first order approximation, to the change in the concentration integral in observation direction.

Best measuring conditions are provided, therefore, if molecular diffusion in x direction may be excluded. In this case, concentration is uniform in x direction and the concentration integral is nothing else than the product of the crystal thickness L and the concentration c. In this overview, we shall benefit from this simplification by considering only channel networks in one and two dimensions.

The spatial resolution in the plane perpendicular to observation is limited by the resolution of optical microscopy, resulting in a minimum pixel size of $\Delta y \times \Delta z \approx 0.5\ \mu\mathrm{m} \times 0.5\ \mu\mathrm{m}$. In the present studies, we have used a Carl-Zeiss JENAPOL interference microscope with a Mach-Zehnder type interferometer (Heinke et al. 2007a; Karge and Kärger

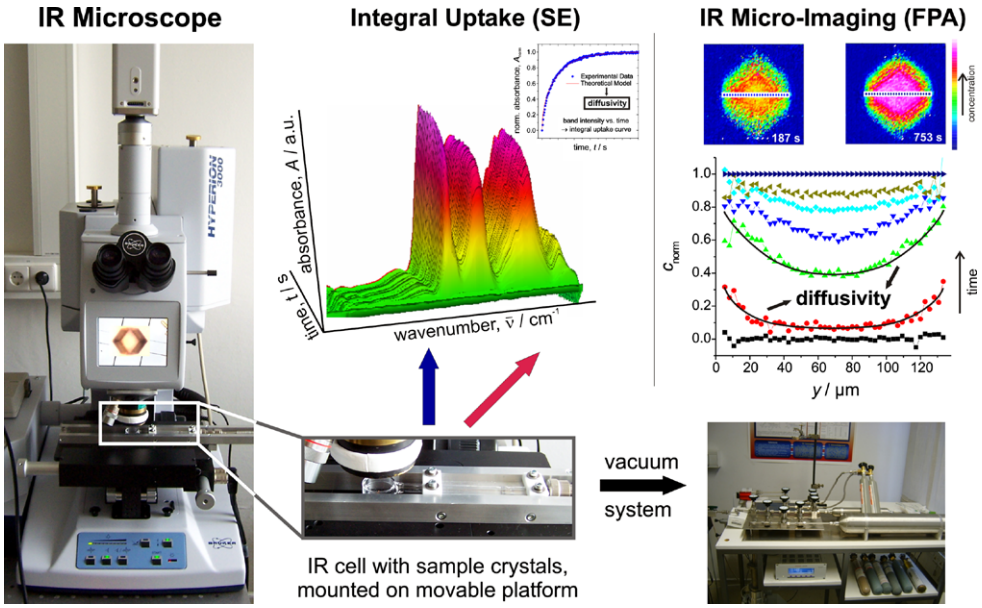

Fig. 2 Experimental set-up and basic principle of the IR microscopy technique. The optical cell is connected to a vacuum system and mounted on a movable platform under the microscope. Only one individual crystal is selected for the measurement. Changes in area under IR bands of the guest species are related to the guest concentration. The spectra can be recorded as signal integrated over the whole crystal (*SE*—single-element detector) or with a special resolution of up to 2.7 µm by the imaging detector (*FPA*—focal plane array)

2008). The minimum temporal separation between two subsequent concentration profiles as presently accessible is 10 s, but there are no fundamental limitations towards smaller time intervals of observation.

2.2 Infrared microscopy (IRM)

Infrared microscopy (IRM), also referred to as IR micro-imaging, is based on the frequency-dependent absorption of infrared light. The setup used in our studies (Fig. 2) makes use of a Fourier-Transform IR microscope (Bruker Hyperion 3000 (Heinke et al. 2007a)) composed of a spectrometer (Bruker Vertex 80v) (Griffiths and de Haseth 1986; Karge and Kärger 2008) and a microscope with a Focal Plane Array detector (Roggo et al. 2005) as the device for micro-imaging. It consists of 128×128 single detectors with a size of 40 µm × 40 µm each. By means of a 15× objective, in the focal plane, i.e., at the position of the crystal under study, a resolution of 2.7 µm × 2.7 µm is gained.

The intensity of the IR light is recorded as a function of the wave length, yielding the "transmission spectrum". According to the Lambert-Beer law, molecular concentration is given by the intensity of a characteristic "absorption band" of this molecule, defined as the negative logarithm of the ratio between the transmission spectrum of the sample over the relevant frequency range and the corresponding background signal. By comparison with a standard, even the absolute number of molecules can be determined. This option of quantitation and the possibility of a simultaneous and selective measurement of different molecular species, e.g. in a mixture, are not provided by interference microscopy, making these two techniques complementary. The possibility to discriminate between different species allows the application of IRM to both uptake and release and to tracer exchange experiments, i.e. to the measurement of transport diffusion and self-diffusion under comparable experimental conditions.

2.3 Data analysis

As an example, Fig. 3 shows the transient concentration profiles of methanol in zeolite ferrierite recorded by interference microscopy during the molecular uptake initiated by a pressure step from 0 to 5 mbar methanol in the surrounding atmosphere (Kärger et al. 2006; Kortunov et al. 2006). Further details of the experiments with this system will be presented in Sect. 3. Here, we will only use these profiles to illustrate the way in which the transient profiles may be used to determine the key data of molecular transport.

The diffusion coefficient of the guest molecules (their "diffusivity") results, via Fick's 1st law, as the factor of proportionality between the molecular fluxes and the concentration gradients, by which they are generated

$$j(x) = -D_{\mathrm{T}}(c(x))\frac{\partial c}{\partial x}. \tag{1}$$

For convenience, we stick to the convention to consider one-dimensional diffusion to occur in the x direction (which in Fig. 3 and most of our other figures happens to be the (arbitrarily chosen) y direction). In the given form, (1) refers to net fluxes which are associated with molecular mass transport. The corresponding diffusivity is therefore referred to as the transport diffusivity (D_{T}).

A similar relation may be noted if one considers the flux of labelled molecules brought about by a gradient in the concentration of the labelled molecules, with the total concentration (i.e. the concentration of the labelled plus the unlabelled molecules) uniform all over the sample. In this case,

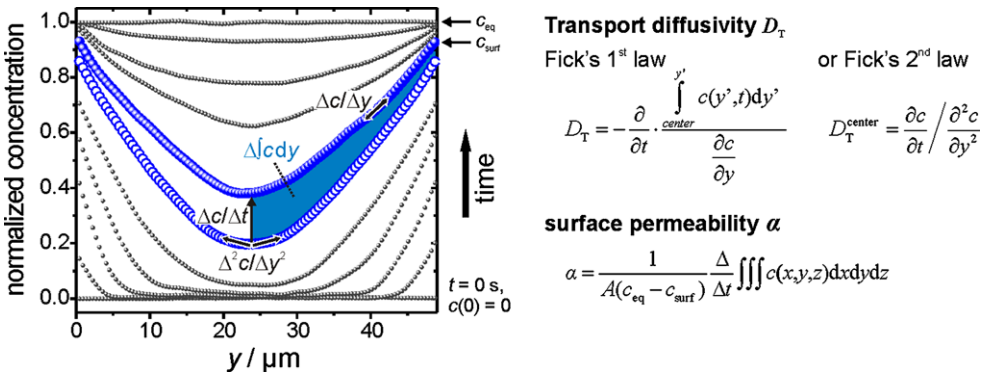

Fig. 3 Data analysis of transient concentration profiles illustrated for the example of methanol uptake in ferrierite (pressure step 0 → 5 mbar in the gas phase, 298 K). The transport parameters can be calculated directly from the profiles by the indicated relations, as well as by fitting with numerical solutions of Fick's laws

the resulting diffusivity (D) is referred to as the tracer diffusivity or self-diffusivity.

In general the concentration at the crystal boundary cannot be expected to assume instantaneously the value which would result under equilibrium conditions with the surrounding guest pressure: additional surface transport resistances may reduce the rate of equilibration. This effect may be taken into account by introducing a (finite) surface permeability α via the relation (Crank 1975; Heinke et al. 2007b)

$$j_{\text{boundary}}(t) = \alpha(c_{\text{eq}} - c_{\text{boundary}}(t)). \tag{2}$$

In analogy to the diffusivities, two types of permeabilities have to be considered, namely those, determined in conventional transient experiments (which would correspond to the transport diffusivities) and those from tracer exchange (corresponding to the tracer or self-diffusivities). The corresponding nomenclature as required by the novel options of measurement, is not yet established.

All data which are necessary for the determination of the relevant quantities via (1) and (2) may be taken from the representations of Fig. 3. The fluxes, in particular, result as the area circumscribed by the c values of two concentration profiles at subsequent instants of time and the two vertical lines passing, respectively, the relevant x value (with, e.g., $x = 0$ to determine the flux through the boundary as relevant for (2)) and the crystal centre (in the considered example, $x = 25$ µm), divided by the spacing Δt between these two instants of time.

In principle, the diffusivity may also be determined on the basis of Fick's 2nd law:

$$\frac{\partial c}{\partial t} = \frac{\partial}{\partial x}\left[D(c(x))\frac{\partial c}{\partial x}\right] = D(c(x))\frac{\partial^2 c}{\partial x^2} + \frac{\partial D(c(x))}{\partial c}\left(\frac{\partial c}{\partial x}\right)^2 \tag{3}$$

In this case, the evaluation is exclusively based on the evolution of local concentrations and there is no need for flux evaluation. One has to be aware, however, that, in the case of transport diffusion, the diffusivity may vary with the concentration. In general, (3) contains therefore two unknown expressions, namely $D(c(x))$ and $\frac{\partial D(c(x))}{\partial c}$, which notably complicates the data analysis. However, at the centre of the crystal (in the considered example, $x = 25$ µm) the concentration profile passes through a minimum (where $(\frac{\partial c}{\partial x}) = 0$), and at this point the disturbing second term vanishes. Hence, at this point, (3) may be applied in a straightforward way, as also indicated in Fig. 3.

The situation is totally different, however, in the case of tracer-diffusion. Here, the self-diffusivity is a function of the total concentration, i.e. of the sum of the concentrations of the labelled and unlabelled molecules. This sum, and hence also the diffusivity, is uniform over the sample. The second term in the second equation may therefore always be omitted, allowing a straightforward determination of the diffusivities on the basis of Fick's 2nd law.

3 Methanol diffusion in ferrierite

Figure 4 shows, in an overview, the scheme of the crystal under study and the concentration profiles (Kärger et al. 2006; Kortunov et al. 2006), observed during molecular uptake of methanol by zeolite ferrierite. It turned out that, after any arbitrary pressure step, the concentration in the roof-like parts of the crystals essentially instantaneously assumed the new equilibrium value. Subtracting these concentrations from overall uptake or release yielded the unexpected result (Kärger et al. 2006; Kortunov et al. 2006) that the two-dimensional array of channels was mainly filled via the smaller channels (in y direction) rather than by the larger ones (in z direction). One has therefore to conclude that the access to the larger channels is blocked, giving rise to profiles which are mainly controlled by one-dimensional diffusion in the y direction (see the examples given in Fig. 3).

The transient concentration profiles of molecular uptake and release observed in these studies (Kärger et al. 2006; Kortunov et al. 2006) provided an unprecedented wealth of information on the transport properties in nanoporous host-guest systems. As an example (Chmelik et al. 2009), Fig. 5

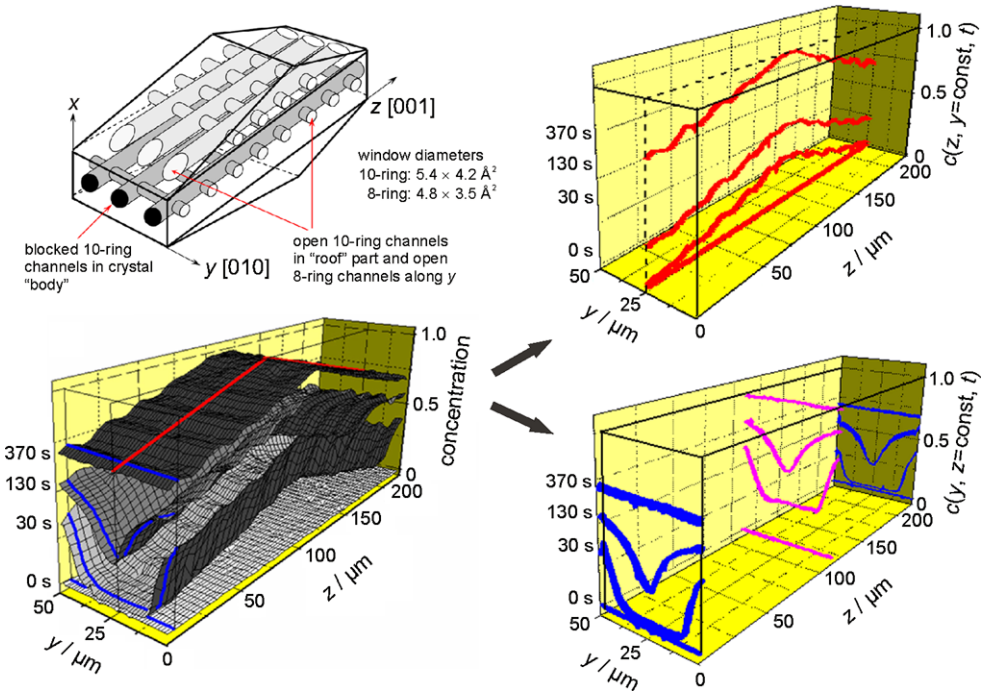

Fig. 4 Transient profiles of methanol concentration for uptake in ferrierite (pressure step 0 → 80 mbar in the gas phase, 298 K). The 1d representations on the right side are extracted from the 2d profiles (lower left corner) for a clearer view on the uptake process. The uptake process is dominated by transport along the smaller 8-ring channels (*y* direction). Except for the formation of a triangular "roof" at early times we find no indications for uptake along *z* direction. Obviously, the larger 10-ring channels are blocked in the crystal "body" and the molecules have to enter through the smaller 8-ring windows in *y* direction (see sketch in the *top left corner*)

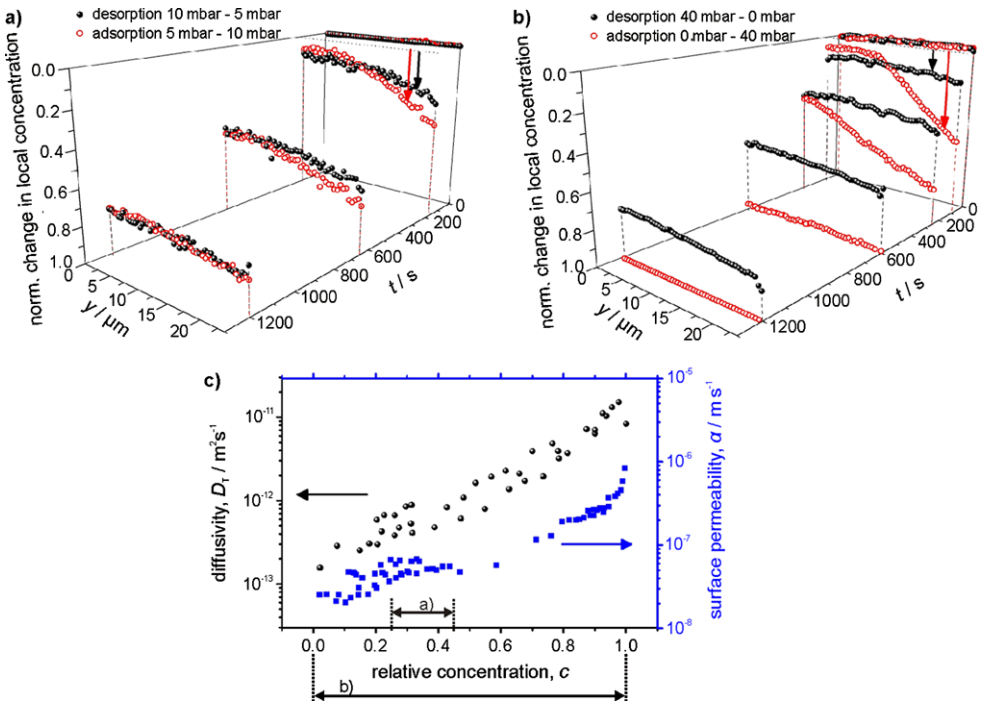

Fig. 5 Methanol in ferrierite: Dramatic impact of the concentration dependence of the transport parameters on molecular uptake (*open spheres*) and release (*full spheres*). (**a**) For small loading steps uptake and release proceed essentially complementary. (**b**) For large loading steps we note a dramatic acceleration of the adsorption. The desorption profiles essentially coincide with those from small loading steps. The "normalized changes in concentration" refer to the initial concentration at time zero. Hence, the adsorption profiles are flipped and can be directly compared with the desorption profiles. (**c**) Transport diffusivity and surface permeability depend strongly on the loading

provides a comparison of the evolution of transient concentration profiles during adsorption and desorption, initiated by a small (a) and by a large (b) pressure step. The concentration range and, hence, the range of diffusivities and permeabilities covered in these experiments, are indicated in Fig. 5c. To facilitate the comparison, the profiles of Figs. 5a and b (showing only one half of the profiles, from the symmetry plane in the centre of the crystals, $y = 0$, to the crystal boundary, $y \approx 23$ µm) are plotted in such a way that they would coincide if the local increase in concentration during adsorption would coincide with the local decrease during desorption. This, clearly, would be the case during tracer exchange: Since the overall concentration has to remain constant the amount of—e.g. labelled—molecules which is adsorbed is equalled by the amount of desorbed (unlabelled) molecules at each position, *y*, and at each instant of time.

This situation is approached by the transient profiles shown in Fig. 5a. With constant diffusivities and permeabilities, (3) is a linear, homogeneous differential equation and the sum of the solutions for uptake and release are a solution again, mimicking the situation of tracer exchange. It is shown by Fig. 5a that, over the considered small range of concentrations, both D and α do not vary appreciably. It is not unexpected, therefore, that the corresponding curves are close to each other.

The larger pressure step, covering diffusivities and permeabilities over close to two orders of magnitude (Fig. 5c), however, leads to dramatic differences. Most interestingly, the desorption rate appears to remain essentially unchanged in comparison with the small pressure step, while the rate of adsorption is found to be dramatically enhanced. Intuitively, this behaviour may be rationalized by realizing that, during uptake, mass transfer through the crystal boundary occurs at the highest loadings, i.e. (see Fig. 5c) with the highest permeabilities and diffusivities and hence, according to (1) and (2) with the highest fluxes. The enhancement of the uptake rate is, therefore, by no means unexpected. During desorption, however, the situation is reversed and mass transfer at the interface between crystallite and surroundings occurs at the lowest loading and, hence, with the lowest diffusivities and permeabilities. In fact, these permeabilities and diffusivities are close to those for a transient sorption experiments with the small pressure step, suggesting the similarity of the respective time constants.

4 Correlating transport diffusion and self-diffusion in MOF ZIF-8

Referring to two different physical situations, namely equilibrium and non-equilibrium measurements, the self-diffusivities and transport diffusivities cannot be expected to be transferred into each other by first principles. However, since both quantities are related to the very fundamental phenomenon of Brownian motion they cannot be expected to be totally uncorrelated. A most useful means for correlating self-diffusivities with transport diffusivities has been provided by the application of the Maxwell-Stefan formalism to diffusion in nanoporous materials (Krishna and van Baten 2007; Seehamart et al. 2009). Following this approach (Paschek and Krishna 2001; Ruthven 2008), the "drag" endured by the guest molecules during self-diffusion (i.e. the reciprocal value of the self-diffusivity) is attributed to two constituents,

$$1/D = 1/D_0 + \theta/Đ_{AA}, \tag{4}$$

resulting from the drag exerted by the pore walls of the host material ($1/D_0$) and from the mutual interaction between the individual diffusants ($\Theta/Đ_{AA}$). In the case of single-file

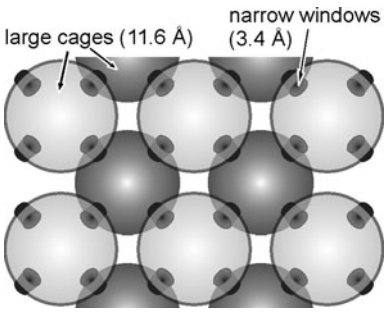

Fig. 6 Schematics of the cubic ZIF-8 structure: Large cages (11.6 Å) connected by narrow windows (3.4 Å)

diffusion (Kärger 2008), e.g., when the molecules are unable to pass each other, this second term becomes infinitely large and prohibits any "normal" diffusion. If, however, molecular propagation is controlled by the passage through the windows between adjacent cavities rather than by any type of "friction" between the different guest molecules, the second term becomes negligibly small. Pore architecture and the structural data of the system under study in this section, as provided by Fig. 6, suggest a situation close to this second limiting case.

The quantity D_0 is referred to as the corrected diffusivity. It is correlated with the transport diffusivity by the relation (Kärger and Ruthven 1992; Paschek and Krishna 2001; Ruthven 2008)

$$D_T = D_0 \frac{d \ln p(c)}{d \ln c} \tag{5}$$

where $p(c)$ denotes the pressure of guest molecules in the surrounding atmosphere which, at equilibrium, keeps the guest concentration within the porous material at c. Thus, in the corrected diffusivity, all driving forces which arise due to non-linearities between guest pressure and concentration (and which do not exist under the conditions of self-diffusion) have been eliminated. Experimentally, the dependence $p(c)$ and, hence, the logarithmic derivative $\frac{d \ln p(c)}{d \ln c}$ (referred to as the thermodynamic factor), is provided by the adsorption isotherms. Owing to the potential of IRM (proportionality between amount adsorbed and signal intensity), we were able to determine the adsorption isotherms directly from our measurements.

So far, comparative studies of self-diffusion and transport diffusion suffered under the deficiencies in their comparability. As the classical example (Kärger and Ruthven 1981, 1989, 1992), PFG NMR followed typically the paths of molecular self-diffusion over distances much smaller than the crystal extensions while, during the classical uptake and release experiments, transport diffusion was followed into or out of the whole crystals. Today, we dispose of persuasive evidence (Vasenkov and Kärger 2002; Feldhoff et al. 2009) that the resistances governing molecular transport over such different space scale may notably

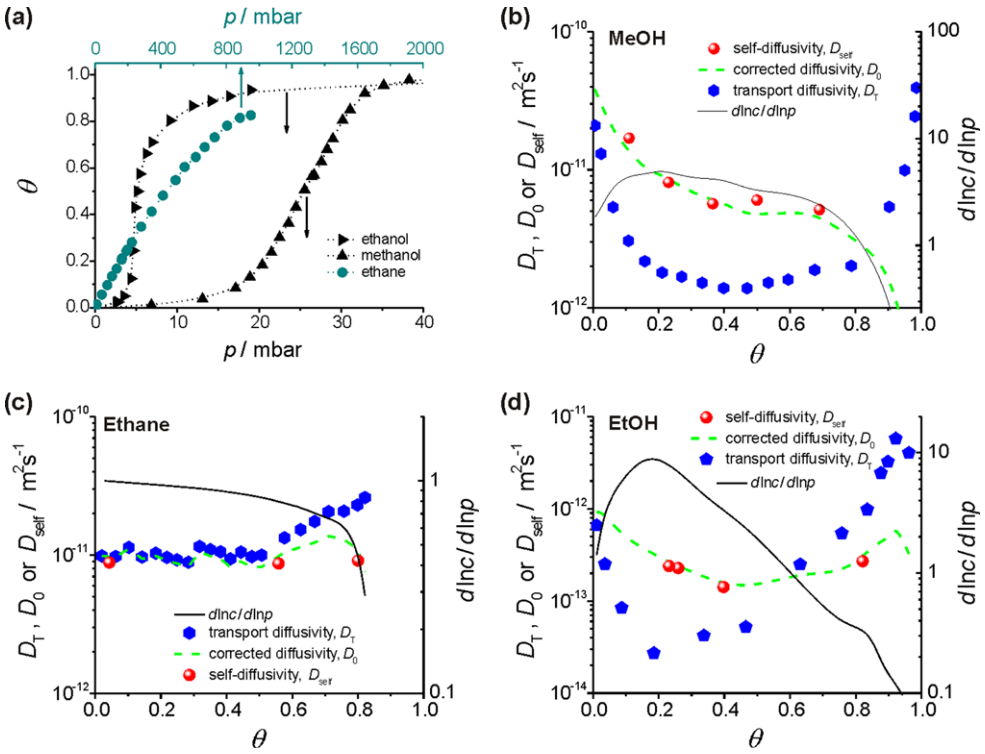

Fig. 7 Methanol, Ethane and Ethanol in ZIF-8 at 298 K. (**a**) The adsorption isotherm of ethane (upper ordinate scale) shows a usual ("type I") behavior, whereas the isotherms of methanol and ethanol (lower ordinate scale) exhibit a pronounced S-shape ("type III"). All isotherms were normalized to reach an occupancy of $\theta = 1$ at saturated vapor pressure. Loading dependence of transport (D_T), corrected (D_0) and self-diffusivity (D_{self}) of (**b**) methanol (MeOH), (**c**) ethane and (**d**) ethanol (EtOH). The *full lines* show the inverse thermodynamic factor as obtained from (**a**)

differ from each other. These differences can lead to substantial differences in the resulting diffusivities! With the advent of IRM, the observation of transport diffusion (by uptake and release experiments) and of self-diffusion (by tracer exchange experiments) has become possible over identical space and time scales. Hence, for the first time a meaningful comparison between diffusion measurements under equilibrium and non-equilibrium has become possible.

Figure 7 provides a summary of our measurements performed with a metal organic framework (MOF) of type ZIF-8 (Chmelik et al. 2010). They include the self-diffusivities and transport diffusivities of methanol (b), ethane (c) and ethanol (d) and their normalized isotherms (a), as well as the derivatives $d\ln c/d\ln p$, resulting from these isotherms, and the corrected diffusivities, calculated via (5) from these derivatives and the transport diffusivities (b–d).

In all cases, the corrected diffusivities are found to nicely agree with the self-diffusivities. Our model assumption that molecular propagation is limited by the passage through the windows between adjacent cavities and that, therefore, the second term on the right side of (4) may be neglected, is thus found to be completely justified. As a most remarkable result, the self-diffusivity of methanol (b) notably exceeds the transport diffusivity. This finding is found to be correlated with the fact that the logarithmic derivative $d\ln c/d\ln p$ attains values which are much larger than one. This result, in turn, is caused by the fact that the mutual interaction between the methanol molecules notably exceeds the strength of interaction with the internal surface of the MOFs under study (type III of the IUPAC classification (Schüth et al. 2002)) approaching the classical situation of water adsorption on hydrophobic surfaces.

Ethane, by contrast, exhibits none of these peculiarities. The isotherm (a) is found to be essentially linear. Only at the highest concentrations considered, the isotherm deviates to smaller values, leading to decreasing values of $d\ln c/d\ln p$. This dependency is exactly reflected by the diffusivities, which are found to be essentially identical ($D_T \approx D \approx D_0$) up to medium concentrations. For higher concentrations, the decrease of $d\ln c/d\ln p$ to values smaller than 1 is nicely reflected by the departure of the transport diffusivities to values above the self-diffusivities (and corrected diffusivities).

The diffusivities of ethanol (Fig. 7d) are found to reflect features of both methanol and ethane. In the range of smaller loadings, the adsorption isotherm reflects the dominating influence of the mutual interaction of the ethanol molecules which, like with methanol, results in self-diffusivities notably exceeding the transport diffusivity. This situation is found to be reversed for loadings in the last quarter of pore filling where the adsorption isotherm approaches the shape of the Langmuir isotherm, yielding values $d\ln c/d\ln p < 1$, resulting in transport diffusivities exceeding the self-(and corrected) diffusivities.

5 Conclusion

With the introduction of interference microscopy (IFM) and IR microscopy (or IR micro-imaging, IRM) sorption sci-

ence has been reinforced by two powerful new tools, enabling the observation of the evolution of the distribution of guest molecules inside nanoporous materials. Analysis of these profiles allows, for the first time, the *microscopic* determination of diffusivities and surface permeabilities under non-equilibrium conditions. Moreover, transport diffusivities and self-diffusivities can be observed under absolutely comparable conditions. These novel options have been highlighted by demonstrating the great relevance of the pressure step during transient sorption experiments on the relation of the transient concentration profiles during adsorption and desorption. Considering a member of the new family of metal-organic frameworks (MOFs), for the first time absolute compatibility between transport diffusivities and self-diffusivities could be demonstrated. In view of the ongoing dramatic enlargement of the spectrum of nanoporous materials, the wealth of options provided by the novel measuring techniques is scarcely predictable. The investigation of multi-component systems, including chemical conversions, will, most likely, be among the future highlights of such investigations.

Acknowledgements We dedicate this paper to Professor Douglas M. Ruthven on the occasion of his 70th birthday. The authors owe a special debt of gratitude to Professor Ruthven for numerous occasions of stimulating and fruitful scientific exchange and a most successful collaboration in many research projects.

We are obliged to Sergey Vasenkov, Pavel Kortunov, Lars Heinke, Despina Tzoulaki for their work and discussion on the presented diffusion studies in ferrierite. We also want to thank Jürgen Caro and Jing Li for synthesizing and providing the nanoporous crystals.

Financial support by Deutsche Forschungsgemeinschaft (International Research Group "Diffusion in Zeolites", International Research Training Group "Diffusion in Porous Materials" and DFG research group "From local constraints to macroscopic transport") and Fonds der Chemischen Industrie is gratefully acknowledged.

References

Bär, N.-K., Balcom, B.J., Ruthven, D.M.: Direct measurement of transient concentration profiles in molecular sieve particles and columns by MRI. In: Do, D.D. (ed.) Adsorption Science and Technology, pp. 6–13. World Scientific, Singapore (2000)

Bär, N.K., Bauer, F., Ruthven, D.M., Balcom, B.J.: Direct and indirect observation of coke deposits on HZSM-5 by ^{1}H NMR imaging. J. Catal. **208**, 224–228 (2002)

Chmelik, C.: FTIR microscopy as a tool for studying molecular transport in zeolites. PhD thesis, Leipzig University, Leipzig (2007)

Chmelik, C., Kortunov, P., Vasenkov, S., Kärger, J.: Internal transport resistances and their influence on diffusion in zeolites as traced by microscopic measuring techniques. Adsorption **11**, 455–460 (2005)

Chmelik, C., Heinke, L., Kortunov, P., Li, J., Olson, D., Tzoulaki, D., Weitkamp, J., Kärger, J.: Ensemble measurement of diffusion: novel beauty and evidence. Chem. Phys. Chem. **10**, 2623–2627 (2009)

Chmelik, C., Bux, H., Caro, J., Heinke, L., Hibbe, F., Titze, T., Kärger, J.: Mass transfer in a nanoscale material enhanced by an opposing flux. Phys. Rev. Lett. **104**, 085902 (2010)

Crank, J.: The Mathematics of Diffusion. Clarendon Press, Oxford (1975)

Feldhoff, A., Caro, J., Jobic, H., Krause, C.B., Galvosas, P., Kärger, J.: Direct evidence of intracrystalline transport resistances in nanoporous zeolite NaX. Nature Chem. (2009, submitted)

Griffiths, P.R., de Haseth, J.A. Fourier Transform Infrared Spectroscopy. Wiley, New York (1986)

Heink, W., Kärger, J., Pfeifer, H.: Application of zeugmathography to study kinetics of physical adsorption. Chem. Eng. Sci. **33**, 1019–1023 (1978)

Heinke, L., Chmelik, C., Kortunov, P., Ruthven, D.M., Shah, D.B., Vasenkov, S., Kärger, J.: Application of interference microscopy and IR microscopy for characterizing and investigating mass transport in nanoporous materials. Chem. Eng. Technol. **30**, 995–1002 (2007a)

Heinke, L., Kortunov, P., Tzoulaki, D., Kärger, J.: Exchange dynamics at the interface of nanoporous materials with their surroundings. Phys. Rev. Lett. **99**, 228301 (2007b)

Jobic, H., Theodorou, D.: Quasi-elastic neutron scattering and molecular dynamics simulations as complementary techniques for studying diffusion in zeolites. Microporous Mesoporous Mater. **102**, 21–50 (2007)

Karge, H.G., Kärger, J.: Application of IR spectroscopy, IR microscopy, and optical interference microscopy to diffusion in zeolites. In: Karge, H.G., Weitkamp, J. (eds.) Adsorption and Diffusion, pp. 135–206. Springer, Berlin, Heidelberg (2008)

Kärger, J.: Single-file diffusion in zeolites. In: Karge, H.G., Weitkamp, J. (eds.) Molecular Sieves, Science and Technology: Adsorption and Diffusion, pp. 329–366. Springer, Berlin, (2008)

Kärger, J., Caro, J.: Interpretation and correlation of zeolitic diffusivities obtained from nuclear magnetic resonance and sorption experiments. J. Chem. Soc. Faraday Trans. I **73**, 1363–1376 (1977)

Kärger, J., Ruthven, D.M.: Diffusion in zeolites. J. Chem. Soc. Faraday Trans. I **77**, 1485–1496 (1981)

Kärger, J., Ruthven, D.M.: On the comparison between macroscopic and NMR measurements of intracrystalline diffusion in zeolites. Zeolites **9**, 267–281 (1989)

Kärger, J., Ruthven, D.M.: Diffusion in Zeolites and Other Microporous Solids. Wiley, New York (1992)

Kärger, J., Kortunov, P., Vasenkov, S., Heinke, L., Shah, D.B., Rakoczy, R.A., Traa, Y., Weitkamp, J.: Unprecedented insight into diffusion by monitoring concentration of guest molecules in nanoporous host materials. Angew. Chem. Int. Ed. **45**, 7846–7849 (2006)

Kortunov, P., Heinke, L., Vasenkov, S., Chmelik, C., Shah, D.B., Kärger, J., Rakoczy, R.A., Traa, Y., Weitkamp, J.: Internal concentration gradients of guest molecules in nanoporous host materials: measurement and microscopic analysis. J. Phys. Chem. B **110**, 23821–23828 (2006)

Krishna, R., van Baten, J.M.: Insights into diffusion of gases in zeolites gained from molecular dynamics simulations. Microporous Mesoporous Mater. **109**, 91–108 (2007)

Paschek, D., Krishna, R.: Kinetic Monte Carlo simulations of transport diffusivities of binary mixtures in zeolites. Phys. Chem. Chem. Phys. **3**, 3185–3191 (2001)

Roggo, Y., Edmond, A., Chalus, P., Ulmschneider, M.: Infrared hyperspectral imaging for qualitative analysis of pharmaceutical solid forms. Anal. Chim. Acta **535**, 79–87 (2005)

Ruthven, D.M.: Fundamentals of adsorption equilibrium and kinetics in microporous solids. In: Karge, H.G., Weitkamp, J. (eds.) Molecular Sieves—Science and Technology: Adsorption and Diffusion, pp. 1–43. Springer, Berlin, Heidelberg, (2008)

Schemmert, U., Kärger, J., Krause, C., Rakoczy, R.A., Weitkamp, J.: Monitoring the evolution of intracrystalline concentration. Europhys. Lett. **46**, 204–210 (1999a)

Schemmert, U., Kärger, J., Weitkamp, J.: Interference microscopy as a technique for directly measuring intracrystalline transport diffusion in zeolites. Microporous Mesoporous Mater. **32**, 101–110 (1999b)

Schüth, F., Sing, K.S.W., Weitkamp, J.: Handbook of Porous Solids. Wiley-VCH, Weinheim (2002)

Seehamart, K., Nanok, T., Krishna, R., Baten, J.M.v., Remsungnen, T., Fritzsche, S.: A molecular dynamics investigation of the influence of framework flexibility on self-diffusivity of ethane in Zn(tbip) frameworks. Microporous Mesoporous Mater. **125**, 97–100 (2009)

Vasenkov, S., Kärger, J.: Evidence for the existence of intracrystalline transport barriers in MFI-type zeolites: a model consistency check using MC simulations. Microporous Mesoporous Mater. **55**, 139–145 (2002)